Observed Evidence of Springtime Cloud Influence on Regional Climate and its Implication in Runoff Decline in Upper Colorado River Basin

Yun Lin[1], Yoshihide Takano[2], Yu Gu[3], jingyu wang[4], Bin Zhao[5], Kuo-Nan Liou[2], and Rong Fu[1]

[1]University of California, Los Angeles
[2]University of California Los Angeles
[3]Joint Institute for Regional Earth System Science and Engineering
[4]Pacific Northwest National Laboratory
[5]Tsinghua University

November 24, 2022

Abstract

The sub-seasonal features of the annual trends of runoff and other associated hydroclimatic variables in the upper Colorado River basin (UCRB) are examined using multiple datasets from in-situ observations, reanalysis, and modeling for early spring (February, March, and April), given that about 58% of annual mean runoff decline from 1980 to 2018 stem from its decreases in the three months. Our analysis suggests that the strong annual trends of hydroclimatic variables in March are more statistically significant than other two months. While recent observational studies attribute the declining runoff to regional warming and precipitation decrease, we suggested, for the first time, that a larger decreasing trend of the runoff in March is caused by the declining cloud optical depth which induces further decrease in precipitation and additional increase in temperature on top of climatic warming. The recent cloud suppression likely results from stronger subsidence and larger moisture flux divergence over southwestern United States because of abnormal circulation patterns in varying climate, in turn leading to drier atmosphere which is unfavorable for cloud formation/development over the UCRB region. The cloud influence on the runoff in March in the UCRB observed in this study implies the importance of understanding sub-seasonal variations of hydroclimate in the changing climate, as well as a need of future studies on the response of circulation patterns to climate change at sub-seasonal level and its implication on local hydroclimate.

Hosted file

`cloud_influence_on_runoff_20210929_si.docx` available at https://authorea.com/users/548836/articles/603267-observed-evidence-of-springtime-cloud-influence-on-regional-climate-and-its-implication-in-runoff-decline-in-upper-colorado-river-basin

Hosted file

`essoar.10508226.1.docx` available at https://authorea.com/users/548836/articles/603267-observed-evidence-of-springtime-cloud-influence-on-regional-climate-and-its-implication-in-runoff-decline-in-upper-colorado-river-basin

Yun Lin[1,*], Yoshihide Takano[1,*], Yu Gu[1], Jingyu Wang[2], Bin Zhao[3], Kuo-Nan Liou[1, †], and Rong Fu[1]

1 Department of Atmospheric and Oceanic Sciences, Joint Institute for Regional Earth System Science and Engineering, University of California, Los Angeles, California 90095 USA

2 Atmospheric Sciences and Global Change Division, Pacific Northwest National Laboratory, Richland, WA 99352

3 School of Environment and State Key Joint Laboratory of Environment Simulation and Pollution Control, Tsinghua University, Beijing 100084, China

Corresponding author: Yun Lin (`yunlin@g.ucla.edu`)

[*] Yun Lin and Yoshihide Takano contributed equally to this paper.

[†] Deceased.

Key points

- Hydroclimatic annual trend in the UCRB shows sub-seasonal feature in early spring.

- Thinner clouds spur extra warming and thereby additional runoff decline in March.

- Intensified large-scale subsidence leads to dryness and cloud suppression in March.

Abstract

The sub-seasonal features of the annual trends of runoff and other associated hydroclimatic variables in the upper Colorado River basin (UCRB) are examined using multiple datasets from in-situ observations, reanalysis, and modeling for early spring (February, March, and April), given that about 58% of annual mean runoff decline from 1980 to 2018 stem from its decreases in the three months. Our analysis suggests that the strong annual trends of hydroclimatic variables in March are more statistically significant than other two months. While recent observational studies attribute the declining runoff to regional warming and precipitation decrease, we suggested, for the first time, that a larger decreasing trend of the runoff in March is caused by the declining cloud optical depth which induces further decrease in precipitation and additional increase in temperature on top of climatic warming. The recent cloud suppression likely results from stronger subsidence and larger moisture flux divergence over southwestern United States because of abnormal circulation patterns in varying climate, in turn leading to drier atmosphere which is unfavorable for cloud formation/development over the UCRB region. The cloud influence on the runoff

in March in the UCRB observed in this study implies the importance of understanding sub-seasonal variations of hydroclimate in the changing climate, as well as a need of future studies on the response of circulation patterns to climate change at sub-seasonal level and its implication on local hydroclimate.

1. Introduction

Runoff of the upper Colorado River basin (UCRB) is vital to water supply in the United States Southwest and California, but it is especially vulnerable to climate change because of the snowmelt-dominated water supply in the basin [*Hock*, 2019]. The recent decline of the UCRB runoff has been wildly related to precipitation deficits and rising temperatures under anthropogenic climate change, with the relative importance of different drivers varying with time periods examined and methodologies used [*Hoerling et al.*, 2019; *McCabe et al.*, 2017; *Udall and Overpeck*, 2017; *Vano et al.*, 2012; *Vano and Lettenmaier*, 2014; *Woodhouse et al.*, 2016; *Xiao et al.*, 2018]. Previous estimations based on instrumental records have documented that most of annual variations of streamflow are explained by precipitation variability in river basins across the western U.S., suggesting the dominant role of precipitation anomalies relative to temperature changes in determining runoff trends [*Gleick*, 1986; *Karl and Riebsame*, 1989; *Nash and Gleick*, 1991; *Wigley and Jones*, 1985]. For example, it is documented that precipitation deficit is the major cause of the midcentury drought in 1950s (Udall and Overpeck 2017). On the other hand, temperature warming tends to either moderate or exacerbate the influence of precipitation anomalies, overall playing a secondary role in runoff reductions in the past (Woodhouse et al. 2016). The contributions to the annual runoff reduction due to the temperature rising can be about 5-10%, according to studies of Vano et al. (2012) over 1975-2005 and Udall and Overpeck (2017) over 2000-2014. However, at a longer term (e.g., a 100-year period between 1916-2014), Xiao et al. (2018) found that more than half (53%) of the runoff decreasing trend can be attributed to the warming through hydrologic modeling estimation. They also noted that the precipitation slightly increased (i.e., 1.4%) over this period but with the streamflow decline of 16.5%. In addition, the warming trend over the UCRB is getting pronounced since 1980s [*Dawadi and Ahmad*, 2013; *McCabe et al.*, 2017] and more frequent warmer years with lower flow since 1988 has been reported (Woodhouse et al., 2016), both of which suggests an increasingly importance of rising temperature in more recent years in controlling the response of runoff. For example, both observational and modeling studies have confirmed that the very important role of rising temperature during the ongoing post-Millennium Drought relative to its counterpart in the midcentury drought (Udall and Overpeck 2017; Xiao et al., 2018). Soil moisture is another influential factor for runoff, but its impact on runoff is at lesser degree than that of temperature and precipitation [*Hamlet et al.*, 2007; *Seneviratne et al.*, 2010; *Woodhouse et al.*, 2016].

Given that the possible increasing influence of climate change on runoff, model-

ing efforts have been made in the projections of future changes in temperature and precipitation, as well as their impacts on runoff response. Although the sensitivity of streamflow to precipitation (percent runoff change per percent precipitation change) in future projections is less disputable [*Hobbins and Barsugli*, 2020], the runoff reduction attributable to regional warming (i.e., temperature sensitivity of runoff to temperature, defined by percent discharge change per degree Celsius of warming) shows large variations, ranging from <10 to 45% by 2050 [*Vano and Lettenmaier*, 2014]. The uncertainty is particularly originated from the great discrepancy between empirical-based regressions and hydrologic modeling simulations used to estimate streamflow sensitivity [*McCabe et al.*, 2017; *P. C.D. Milly et al.*, 2018; *Nowak et al.*, 2012; *Vano et al.*, 2012; *Vano and Lettenmaier*, 2014]. Obviously, the current efforts still cannot reconcile each other in streamflow sensitivity estimations. To counter this, more comprehensive process understanding, rigorous synthesis of observations, and modeling works with various model frameworks and full range of temperature perturbation inputs are required. One such study carried out recently by *P C D Milly and Dunne* [2020] has estimated individual contributions of various processes related to climatic warming to the UCRB discharge change, suggesting that the total annual decrease is about 9.3% $°C^{-1}$ and the primary driver of runoff loss is the snow-albedo feedback under the warming climate.

Alternatively, other studies argue that the recent declines of the UCRB runoff could at least partially be attributed to the effect of dust on snowpack [*Painter et al.*, 2010], teleconnections with tropical Pacific sea surface temperature [*Lehner et al.*, 2018; *S Zhao et al.*, 2021], the direct effects of rising CO_2 concentration on the balance of long-wave radiation and on water-use efficiency of vegetation, as well as land-cover modifications due to wildfires and insect outbreaks [*Hobbins and Barsugli*, 2020]. However, all these possible drivers still need further more accurate estimations, particularly together with the direct effect of global warming.

On the other hand, the response of streamflow to temperature change in Western United States is characterized with strong subannual variations [*Ban et al.*, 2020; *Das et al.*, 2011; *Vano and Lettenmaier*, 2014; *Vano et al.*, 2015], and may represent another important source of uncertainties when estimating the sensitivity of annual runoff to regional warming. The examination of sub-annual variations particularly focuses on warm (April to September) and cool (October to March) seasons. For example, Ban et al. (2020) find that there are asymmetrical responses of annual and seasonal streamflow changes to the warming of warm and cool seasons in river basins like the UCRB in Western United States. In addition to the distinct responses of warm and cool seasons, there exist subseasonal variations of annual changing patterns for hydroclimatic variables in the UCRB. For instance, [*Miller and Piechota*, 2008] report that the annual trend signs of temperature, precipitation, and streamflow in the Colorado River Basin highly vary by month. However, the sub-seasonal features of hydroclimate in response to regional warming are still rarely touched, and, as a consequence, their driven factors are not fully recognized yet.

3

In this study, we will combine multiple datasets from in-situ observations, re-analysis, and modeling for the UCRB and perform statistical analysis to understand the hydroclimate in the basin at monthly scale, especially in early spring when snowmelt and runoff mostly occur. We aim to comprehensively assess if there are parameters over global warming induced changes in temperature and precipitation (as well as the related teleconnections) may affect the runoff and other associated hydroclimatic condition in the UCRB. We select the period of 1980-2018 for study because the warming over the UCRB is pronounced since 1980s [*Dawadi and Ahmad*, 2013; *McCabe et al.*, 2017] and the signature of temperature rising in the runoff trend appears more significant over this period relative to prior, evident in the fact that there is enhanced frequency of warmer year with lower flow (Woodhouse et al., 2016). In addition, our focus on the most recent decades may help to better understand the recent relationships among hydroclimatic variables under global warming, which will assist in accurate modeling projections of future runoff response in the UCRB.

2. Material and Methodology

For the data collection and analysis, we focus on the UCRB with a domain of 35°– 43°N, 105.7°– 111°W, which is indicated with a red frame in Figure 1. The monthly hydroclimatic variables and their associated variables used in this study include surface runoff, temperature, precipitation, soil moisture, snow water equivalent (SWE), surface net radiation flux, cloud optical depth (COD), and surface and planetary albedo (ALB) for the period 1980 – 2018 (except 1999 – 2018 for SWE based on its availability). Among these variables examined, temperature, precipitation, and soil moisture are the drivers of runoff response in the changing climate suggested by most previous studies. SWE, surface net radiation flux, and albedo parameters are closely related to water supply in snow-fed basins, and can be directly modulated by hydroclimatic conditions like temperature and precipitation (e.g., Hamlet et al. 2007; McCabe et al. 2017; Milly and Dunne, 2021). The COD is selected to probe the possible effects due to cloudiness changes on shortwave radiation attenuation, and thus surface thermodynamic conditions (Hamlet et al., 2007; Vano et al., 2012; Udall and Overpeck, 2017). Surface runoff data was extracted from Global Land Data Assimilation System (GLDAS); station surface temperature was obtained through World Meteorological Organization KNMI Climate Explorer; precipitation and soil moisture were from Climate Prediction Center (CPC), following the recommendation by *Smith and Kummerow* [2013]; the reanalysis data of surface shortwave (SW) and longwave (LW) radiative fluxes, COD, and ALB were extracted from Modern-Era Retrospective analysis for Research and Applications, Version 2 (MERRA2); and SWE was from Canadian Meteorological Centre (CMC). Other variables used for large-scale circulation pattern analysis include three dimensional 500 hPa geopotential height, temperature, relative humidity, water vapor, and wind speeds are all extracted from MERRA2. For the gridded dataset, each variable is averaged over the grid points within the

UCRB. By doing so, the basinwide mean COD can represent the cloudiness in the UCRB to some extent because the average is done over all the grid elements unconditionally in the basin (including cloudy and non-cloudy elements). The non-gridded temperature data is averaged over all stations inside the domain. All the datasets used in this study are also listed in Table S1 with the information on spatial resolutions and accessible online sources.

Yearly time series for monthly mean of each hydroclimatic variable were subjected to statistical analysis using Mann-Kendall test in an attempt to detect the sub-seasonal characteristics of their annual trends between 1980 and 2018. The Mann-Kendall test is a nonparametric test and does not require the normality of the dataset, and thereby is popular for the trend analysis in climatologic and in hydrologic time series [*Mavromatis and Stathis*, 2011; *Yue and Wang*, 2004]. Another advantage of the Mann-Kendall test is its insensitivity to abrupt breaks caused by inhomogeneous time series. Throughout the analysis, the Mann–Kendall trend significance test was accessed at the significance level at 0.05 and/or 0.1. The Theil-Sen slopes were derived for denoting the trending intensity.

Figure 1 Map of upper Colorado River basin (UCRB). A red frame indicates

the investigated domain: 35-43° N, 105.7-111° W. (USGS, 2018).

Pearson's correlation analysis was performed to evaluate the associations between two interested hydroclimatic variables. Partial correlation coefficient is a measure of the dependence between two variables when the influence of possible controlling variables is removed [*Engström and Ekman*, 2010; *Hardle and Simar*, 2015; *Johnson and Wichern*, 2007; *B Zhao et al.*, 2018], we also conducted partial correlation analysis following [*Engström and Ekman*, 2010] for runoff with temperature and precipitation as the influence of other possible drivers were removed. In addition, the relative contribution of individual predictor (e.g., temperature, precipitation, and so on) to variations of runoff was estimated by performing multiple linear regression analysis. The detailed description about multiple linear regression is in Text S1 and S2.

3. Results

The overall trends are illustrated in the time series of water-year (defined as the 12-month period from October 1 for any given year through September 30 of the following year) annual runoff, temperature, and precipitation in the UCRB (Figure S1). The relative variation of the annual runoff is comparable to the natural flow of Colorado River at Lees Ferry reported by Woodhouse et al. (2016). The UCRB runoff shows a strong decreasing trend from 1980 to 2018, whereas temperature exhibits an increasing trend and no significant trend is on precipitation, suggesting that the decline of runoff is primarily caused by rising temperature. Our results appear more consistent with Xiao et al. (2018)'s study on the period of 1916-2014, in which more than half of the runoff reduction is attributed to temperature warming, but different from others [*Gleick*, 1986; *Karl and Riebsame*, 1989; *McCabe et al.*, 2017; *Nash and Gleick*, 1991; *Udall and Overpeck*, 2017; *Vano et al.*, 2012; *Wigley and Jones*, 1985], in which the negative precipitation anomalies are the main driver of runoff decline, with a minor role of temperature changes. The two reasons below could be responsible for the inconsistency between our results with others: Firstly, our study focus on the most recent period with more pronounced warming than that in other studies (e.g., 1975-2005 in Vano et al. (2012)), and thereby the temperature is likely more influential in our study. This is also revealed by Woodhouse et al. (2016); Secondly, the great interannual variation of precipitation over the studying period likely leads to a difficulty to recognize the signature of precipitation changing in the runoff trend. However, the changes in precipitation did contribute to the runoff variation during this period, which is evident in the fact that the low runoff since 2000 (i.e, the post-Millennium Drought) was well associated with the low level of precipitation over the same period (Figure S1).

To understand the seasonal variations, we examine multiyear monthly means of runoff, temperature, precipitation, and SWE averaged over the UCRB (Figure 2a). The primary peak of runoff occurs in March, while the maximum of SWE occurs in February, one month earlier than the primary peak of runoff. On

6

average, the runoff in February, March, and April together accounts for ~51% of the annual total runoff. Figure 2b shows annual anomalies with respective to the 1980-2018 mean. It is found that the annual total anomalies from 1980 to 2018 are mainly attributed to the changes in early spring, i.e., February, March, and April. Based on the annual trend (i.e., the linear fitting in Figure S1), the difference in annual total runoff between 1980 and 2018 is estimated about -34.7 kg m^{-2}, of which February, March, and April contribute about -7.0, -7.6, and -5.4 kg m^{-2}, respectively. Therefore, there is totally ~58% annual mean loss of runoff from the changes in the three months of early spring. As such, our remaining analysis will focus on the runoff trends and the driving factors in these three months.

Figure 3a shows that the decreasing trends on runoff in all the three months pass the Mann-Kendall significance test (= 0.05), with annual mean rates of -0.16, -0.20, and -0.12 kg m^{-2} yr^{-1} for February, March, and April, respectively. As suggested by previous studies, the strong trends on runoff can be attributed to the variations in temperature, precipitation and soil moisture, which is also evident in Figures 3b-d in this study. The temperature rising (Figure 3b), most likely due to global warming, together with the decreasing of soil moisture (Figure 3d) are responsible for the significant annual loss of runoff for all the three months. However, the runoff decline is moderated by precipitation increase in February and April, leading to weaker runoff trends in these two months than March.
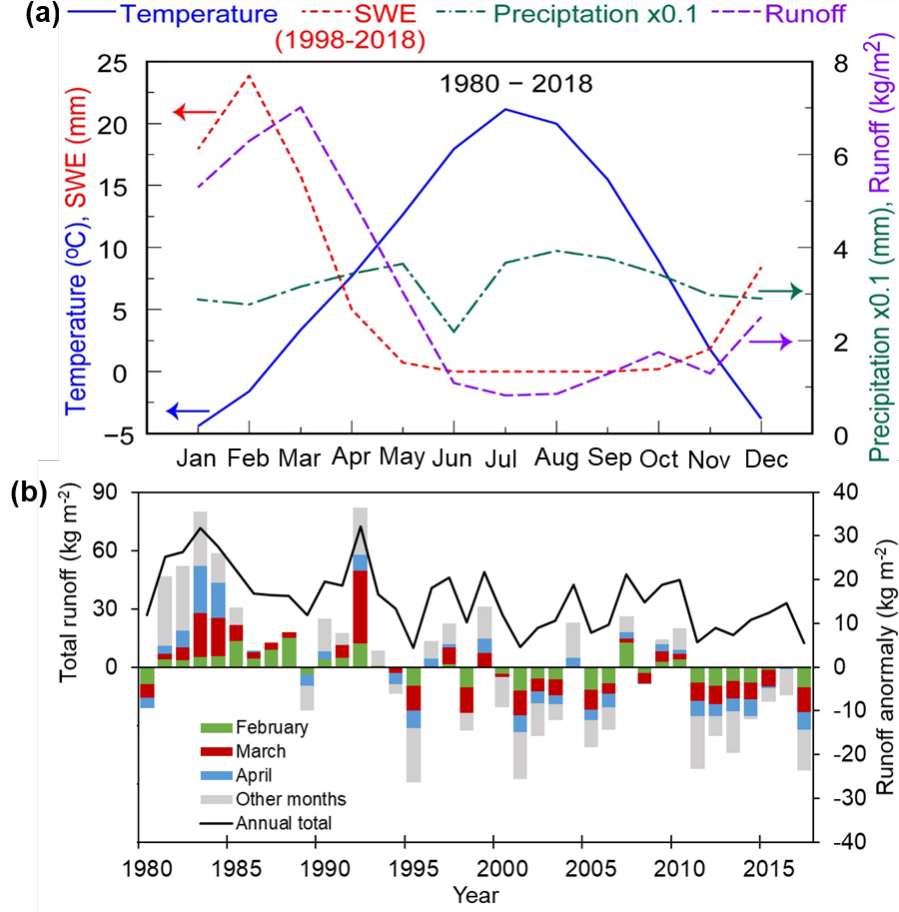
Figure 2 (a) Multiyear monthly mean of runoff, temperature, precipitation, and snow water equivalent (SWE) averaged over the UCRB. The primary runoff peak occurs in March. (b) The time series of annual UCRB runoff curve (left axis) and its anomalies in stack bars (right axis) with respective to (1980-2018) mean. The contributions of February, March, and April to annual total runoff anomaly are marked as green, red, and blue bars, respectively.

It is noteworthy that the runoff in March declines more dramatically than February and April, as indicated by a faster decreasing rate in March than the other two months (Figure 3a). Meanwhile, Figure 3b shows that the warming rate of temperature in March (i.e., 0.05 °C yr^{-1}) is several-time higher than those in February (i.e., 0.02 °C yr^{-1}) and April (i.e., 0.01 °C yr^{-1}). Moreover, the March precipitation shows a decreasing trend with a relatively large rate of 0.4 mm yr^{-1} (Figure 3c), opposite to the slight increasing trends in February and April. Clearly, the combined effect of faster temperature warming and precipitation reduction is responsible for the stronger runoff decreasing in March. Although

runoff is highly correlated with soil moisture in all the three months (Table S2), we can rule out the possibility of soil moisture variability as the primary driving factor for the most significant annual loss in runoff in March, since both the magnitude and the decreasing trend in soil moisture are highly consistent among the three months as shown in Figure 3d.
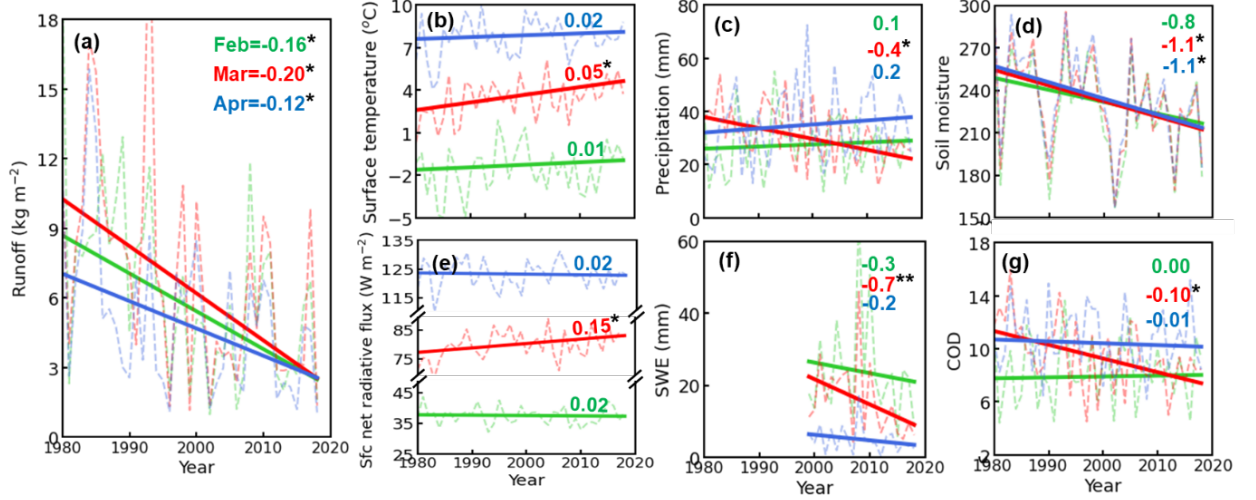
3 Time series of monthly (a) runoff, (b) surface temperature, (c) precipitation, (d) soil moisture, (e) surface net radiative flux, (f) snow water equivalent (SWE), and (g) cloud optical depth (COD), and in the UCRB in February (green dash), March (red dash), and April (blue dash), and their annual trend fittings (thick solid lines) during 1980-2018. Numbers in each panel denote the Theil-Sen slopes of linear fittings, with the asterisks denoting that trends pass the Mann-Kendall trend significance test at the   of 0.05 (*) or 0.10 (**) level.

Another distinct feature of March from February and April is that all the annual trends of the runoff-related hydroclimatic variables examined here, including surface temperature, precipitation, soil moisture, surface net radiative flux, and SWE, pass the Mann-Kendall trend significance test, which is not the case (except soil moisture in April) for February and April. This further confirms that the hydroclimatic condition in March in the UCRB is distinct from February and April, likely stemming from a very different underlying mechanism leading to the runoff decline in March with respective to the other two months.

Given that clouds can regulate the precipitation distribution and provide variable radiative effects, they are an essential link in the global and regional water cycle as well as the energy budget. Therefore, it is very likely that cloud variations may also play a role in sub-seasonal hydroclimatic response. We find that the COD in March presents a very strong, statistically significant decreasing trend, while no such trends are observed in February and April (Figure 3g). The decreasing trend in March is also manifested by the strong positive correlation between COD and runoff with a relatively high correlation coefficient

of 0.40 (Table S2). Since the COD in March is also closely correlated with temperature (R=-0.40) and precipitation (R=0.87), the changes in clouds may contribute to the faster decline of runoff in March by modulating temperature and precipitation. In the following discussions, we will further scrutinize this possible influence on the runoff from cloud.

The relative importance of cloud effect on runoff is evaluated by conducting partial correlation analysis to obtain partial correlation coefficients between runoff and temperature (i.e., $R_{(\mathrm{RO,Temp})\,\mathrm{COD}}$) and precipitation (i.e., $R_{(\mathrm{RO,Preci})\,\mathrm{COD}}$) when the influence of COD is excluded. The results together with regular correlation coefficients ($R_{\mathrm{RO,Temp}}$ and $R_{\mathrm{RO,Preci}}$, respectively) are reported in Table 1. When COD is controlled in regressions for February, the positive correlation between runoff and precipitation ($R_{\mathrm{RO,Preci}}$ = 0.44) becomes weaker ($R_{(\mathrm{RO,Preci})\,\mathrm{COD}}$ = 0.26), but the negative correlation between runoff and temperature ($R_{\mathrm{RO,Temp}}$ = -0.28) gets stronger ($R_{(\mathrm{RO,Temp})\,\mathrm{COD}}$ = -0.36). As such, the opposite effects of cloud on temperature and precipitation cancel each other out, and overall the cloud does not contribute much to the decline of runoff. In April, both $R_{\mathrm{RO,Temp}}$ (-0.54) and $R_{\mathrm{RO,Preci}}$ (0.19) becomes smaller (-0.52 and 0.08, respectively) due to the removal of COD influence, but the changes are relatively small, indicating that the changes in COD might be not the primary driver of the runoff decreasing trend in April. In March, the absolute values of $R_{\mathrm{RO,Temp}}$ (-0.31) and $R_{\mathrm{RO,Preci}}$ (0.38) are both substantially reduced to -0.19 and 0.06, respectively, when COD is controlled, supporting that that the cloud influence is one of the main drivers of the decreasing trend of runoff through causing additional increase in temperature and decrease in precipitation. Further multiple linear regression analysis, as described in Text S1, reveals that COD changes contribute by 25% of the total explainable variation in runoff by regression in March. In contrast, only 6% and 4% of the explainable variations in runoff can be attributed to COD changes in February and April, respectively (Text S2). The multiple regression analysis obtained here also supports more predominant contribution of cloud influence to runoff in March than in February and April, cross-validating the conclusion based on the partial correlation analysis in Table 1.

Table 1 Correlation coefficient and partial correlation coefficient between UCRB variables of runoff (RO), temperature, precipitation, and could optical depth (COD) (1980 − 2018). $R_{\mathrm{A,B}}$ is correlation coefficient between A and B. $R_{(\mathrm{A,B})\,\mathrm{C}}$ is partial correlation coefficient between A and B while controlling the effect of C.

	$R_{\mathrm{RO,Temp}}$	$R_{(\mathrm{RO,Temp})\,\mathrm{COD}}$	$R_{\mathrm{RO,Preci}}$	$R_{(\mathrm{RO,Preci})\,\mathrm{COD}}$
February	-0.28	-0.36	0.44	0.26
March	-0.31	-0.19	0.38	0.06
April	-0.54	-0.52	0.19	0.08

The correlation analysis shows that the COD has a strong negative correlation with the surface net (SW+LW) radiation flux, with correlation coefficients of -0.81, -0.45, and -0.73 for February, March, and April, respectively (Table S2). In other words, the thinner cloud leads to less attenuation of solar radiation and therefore more incoming SW radiation reaching surface. In past several decades, the COD in the UCRB shows a significant decline trend in March, and correspondingly, the surface net radiation flux presents an obvious increasing trend in the same month (Figure 3e). More surface radiation results in additional warming which is evidenced by its strong positive correlation with surface temperature ($R = 0.63$). As a result, the temperature in March warms faster than other two months (Figure 3b), indicating an additional warming due to COD reduction on top of climate warming in March. The enhancement in surface temperature induced by COD reduction can further melt more snow, consistent with the strong decreasing trend on SWE in March (Figure 3f). A warmer temperature can reduce runoff through other pathways, e.g., by spurring evapotranspiration and sublimation and decreasing soil moisture, which has been extensively demonstrated [*Huntington and Billmire*, 2014; *Pascolini-Campbell et al.*, 2021].

On the other hand, strong associations between COD and precipitation are found for all the three months ($R>0.78$), consistent with other studies, e.g., [*Halimi et al.*, 2017; *Mishra*, 2019]. The close co-variation of the two parameters is understandable because COD is proportioned to cloud thickness as a first approximation and the precipitation probability increases as the cloud thickness increases [*Sakakibara*, 1978]. Therefore, the magnitude and the underlying mechanism of the sub-seasonal variation of precipitation in the UCRB can be inferred via the understanding of how the monthly COD changes in past several decades in the same region.

Then another question arises why the March COD in the UCRB is significantly reduced in the past decades while no such trends are found in February and April? This is likely related to the changes in thermodynamic environment in which clouds form. Given that relative humidity (RH) is closely related to cloud formation [*Lamquin et al.*, 2009; *Walcek*, 1994], here we pay appreciable attention to the RH annual trend and its controlling factors to understand the influence of thermodynamic condition on clouds. A strong relationship between COD and RH indeed exists in our study ($R=0.8$, Figure 4a). In addition, we find that the column-mean RH (1000 ~ 300 hPa) during 1980-2018 presents a decreasing trend in all the three months, but only the trend in March is statistically significant, with a much larger slope (i.e., 0.25 % yr^{-1}) than the other two months (i.e., 0.04 % yr^{-1} and 0.10 % yr^{-1} for February and April, respectively, see Figure 4b). Meanwhile, the column-mean air temperature warms at a much higher rate (i.e., 0.07 K yr^{-1}) in March than the other two months (i.e., 0.01 K yr^{-1} and 0.03 K yr^{-1} for February and April, respectively, see Figure 4c). In addition to the warming and drying in March occur in the entire atmosphere column, we separately examined the trends of RH and temperature at different levels as shown in Figure S2, where the strong decreasing/increasing trends of
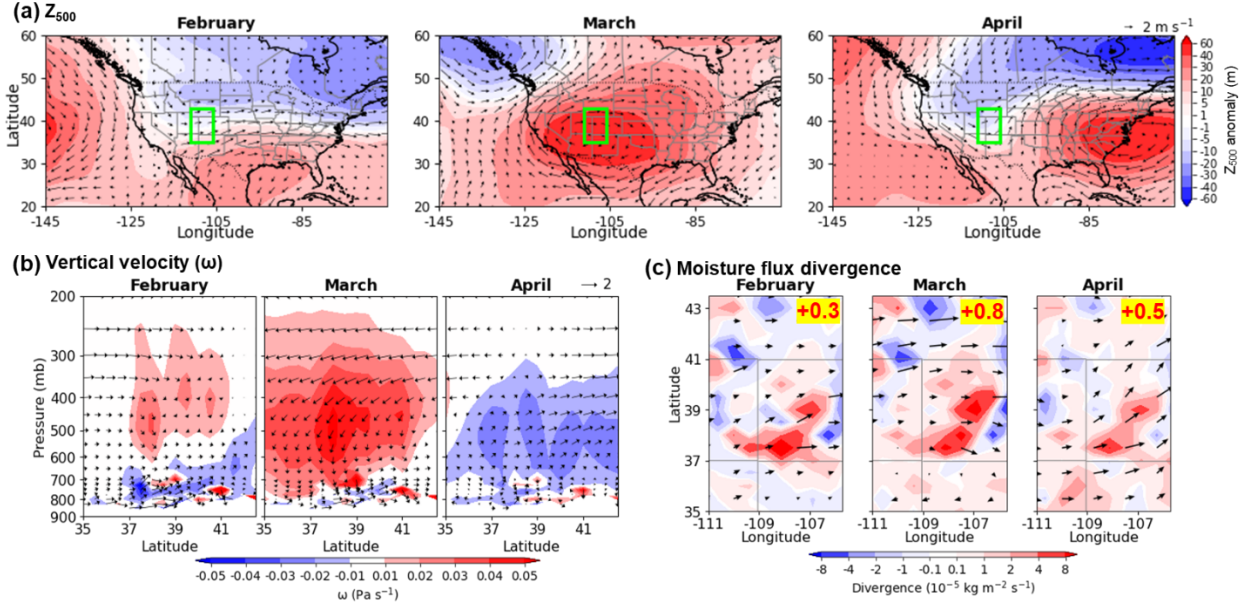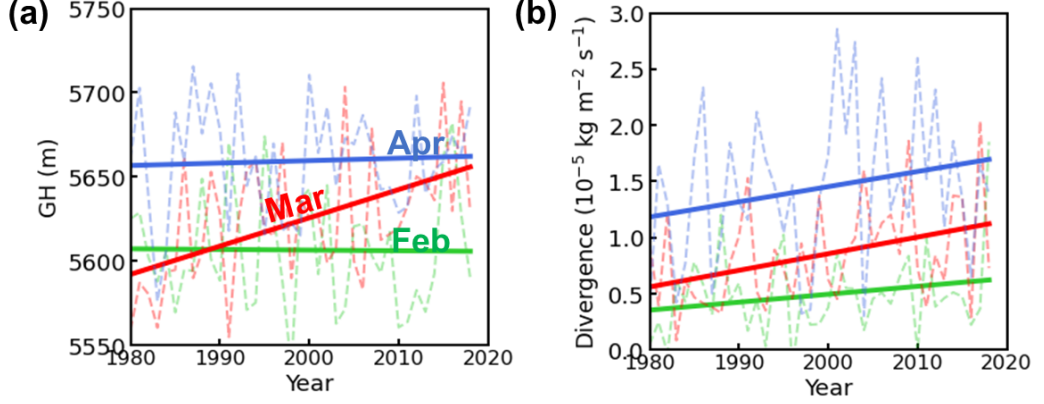
RH/temperature are found at all atmospheric levels.
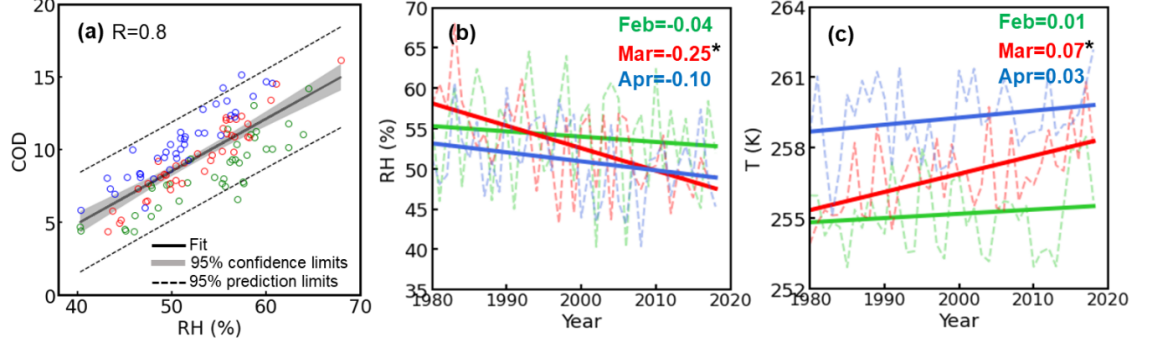
Figure 4 (a) Linear regression between cloud optical depth (COD) and relative humidity (RH) with 95% confidence limits (grey shading) and 95% prediction limits (dash lines), and time series of column mean (1000 ~ 300 hPa) (b) RH and (c) temperature in UCRB in February (green), March (red), and April (blue), and their trends (thick solid lines) for the period 1980 – 2018. Numbers in (b) and (c) denote the Theil-Sen slopes of linear fittings, with the asterisks denoting that the linear trend passes the Mann-Kendall trend significance test at the of 0.05 level. Green, red and blue colors in all panels represent February, March, and April, respectively.

To understand the physics of the distinct sub-seasonal variations of RH and temperature in the UCRB, we further examine monthly changes of large-scale flows in past several decades and their implications for local hydroclimatic condition. Figure 5 depicts the mean differences of mid-atmospheric flow, vertical velocity, and moisture transportation between the last ten years (i.e., 2009-2018) and the first ten years (i.e., 1980-1989) of the study period. The positive 500-hPa geopotential height difference is found in March over the western US region including the UCRB, suggesting that this region is more likely controlled by ridges aloft in recent years. The circulation shows distinct patterns among different months (Figure 5a), as the strong positive anomaly is located west of the UCRB in February, then it propagates right above the UCRB in March, and finally further propagate to the east coast in April. This pattern is also evident in the annual trend analysis, in which the mean 500-hPa geopotential height over the UCRB increases at a much greater rate in March than the other two months (Figure 6a). The ridge control is manifested by strong subsidence as show in Figure 5b middle panel, in contrast to the slight subsidence/ascent patterns found in February/April. The dominant subsidence control in March further constrains the vertical transport of moisture from lower levels, supporting the increased temperature and reduced RH in Figures 4b and c. Regarding the moisture supply advected from regions outside of the UCRB, we find that the vertically integrated (1000 ~ 300 hPa) moisture flux divergence in the UCRB is enhanced in all the three months, indicating that the UCRB is the moisture source rather than the sink in its neighboring area. Moreover, the

domain-averaged enhancement in March (i.e., 0.8×10^{-5} kg m^{-2} s^{-1}) is greater than the other two months (i.e., 0.3×10^{-5} kg m^{-2} s^{-1} and 0.5×10^{-5} kg m^{-2} s^{-1} for February and April, respectively, see Figure 5c). This is in line with the annual trends, showing moisture flux divergence in March increases with a larger slope than that in February and April (Figure 6b). The stronger moisture flux divergence in March reduces the external moist supply and further contributes to the atmosphere drying over the UCRB in addition to the subsidence contribution.

Figure 5 The difference between the last ten years (2009-2018) and the first ten years (1980-1989) in (a) geopotential height at 500 hPa (Z$_{500}$, shading) superimposed with wind vectors at same level, (b) vertical velocity (, shading) along latitude-height cross section over UCRB superimposed with vectors of (V component of wind, -), and (c) vertically integrated moisture flux divergence (1000 ~ 300 hPa, shading) over UCRB domain superimposed with vertically integrated moisture flux (1000 ~ 300 hPa, vectors). The green boxes in (a) mark the UCRB domain, which is domain used for analysis in (b) and (c). From left to right in each panel are February, March and April. The UCRB domain-mean moisture flux divergence for each month is marked in (c), which are yellow-highlighted.

Figure 6 Time series of domain-mean (a) geopotential height at 500 mb and (b) vertically integrated moisture flux divergence over UCRB in February (green dash), March (red dash), and April (blue dash), and their trend (thick solid lines) for the period 1980 − 2018.
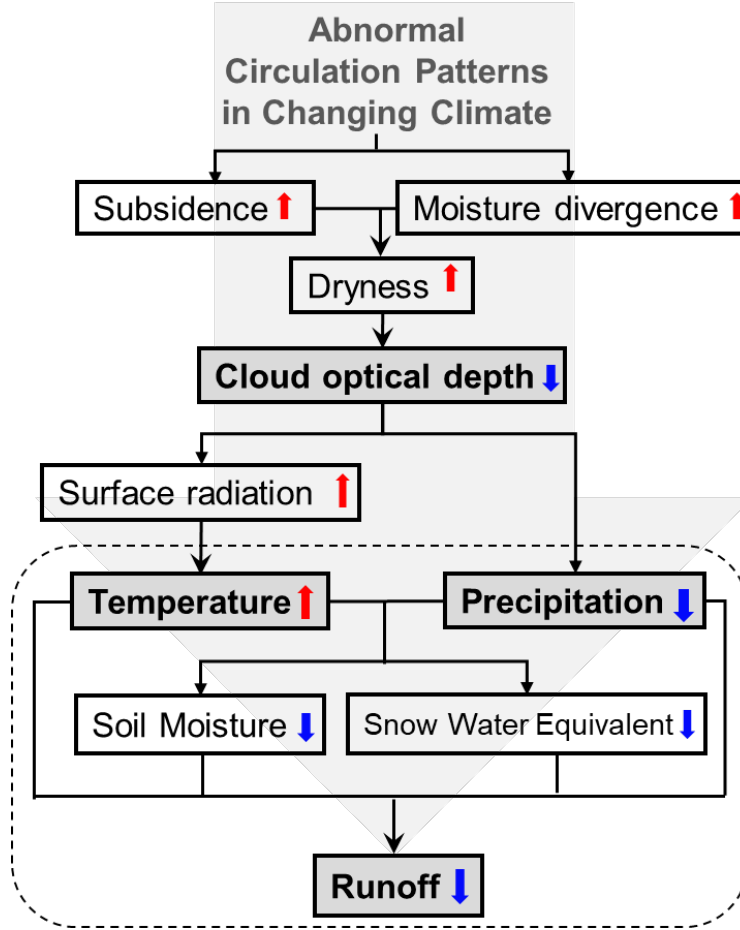
4. Discussion

The flow diagram in Figure 7 summarizes the causative linkage between large-scale air flow perturbations and cloudiness change in March in the UCRB, as well as how this change leads to hydroclimate responses, particularly to the runoff decline. Figure 7 shows that, in March of past several decades, the stronger subsidence and larger moisture divergence were observed in the UCRB likely due to stronger or more persistent the middle-level ridges controlling southwestern US, which in turn results in dryness in the middle and lower atmosphere over the basin. As a result, the cloud formation/development is suppressed, as indicated by the significant reduction in COD, which accompanies less precipitation and solar radiation attenuation. The increased surface solar radiation contributes additional warming at the surface, further reducing the available water supply in the basin for runoff by enhancing evaporation and sublimation, causing drought (e.g., soil moisture deficit), or redistributing SWE to earlier months.

Our explanation by linking the more significant runoff decline in March to the cloud influence can be an important complement to the current understanding of the hydroclimate response in varying climate, in which the runoff decreasing in basins like the UCRB has been wildly attributed to temperature increasing and precipitation decreasing under global warming [*P C D Milly and Dunne*, 2020; *Udall and Overpeck*, 2017; *Woodhouse et al.*, 2016]. To probe the possible sub-seasonal responses of hydroclimate to global warming, we performed additional analysis using the High Resolution WRF Simulations of the Current and Future Climate of North America dataset [*Liu et al.*, 2017], in which two sets of 13-year ensemble simulations with and without of pseudo-global warming

(PGW) were conducted. In comparison to the control simulations, the simulated surface temperature with PGW is enhanced by 4~5 °C in all the three months, and more precipitation is produced in both February and March (Figures S3a and b). Moreover, the total condensate water path in March increases by 10% with PGW relative to the control case (Figure S3c), which is opposite to the decreasing trend of COD suggested above. This suggests that, at least from modeling perspective, the direct effect of climatic warming alone is not able to interpret the distinct sub-seasonal variations of the annual trends on hydroclimatic variables in early spring.

Figure 7 Flow diagram for the causative relationships among large-scale circulation characteristics, cloud optical depth, and hydroclimatic variables (including runoff) in the UCRB in early spring of 1980-2018 (except 1999-2018 for SWE) under varying climate. Red and blue arrows denote increasing and decreasing trends, respectively. The key factors cloud optical depth, temperature, precipitation and runoff are highlighted in bold. The background grey giant arrow

suggests that all the changes are originated from abnormal circulation patterns under changing climate. For February and April, the hydroclimatic response is encompassed in the dashed box, as it starts from variations of surface temperature and precipitation which are likely resulted from climatic warming alone.

A recent study by Milly and Dunne (2020) reveals that the decline of Colorado River flow stemming from enhanced evapotranspiration under global warming is mainly driven by snow-albedo feedback. Our analysis also suggests a weak decreasing trend of surface albedo (Figure S4) along with the continuous snow losses annually (i.e., SWE reduction in Figure 3f) in the three months, supporting that the climatic warming-induced snow-albedo feedback may play a minor role in the water reduction in the UCRB. It is worth noting that the planetary albedo in March exhibits a statistically significant decreasing trend with a much larger slope than the other two months (Figure S5), which cannot be explained by the interannual variations of surface albedo since the similar decreasing trends on surface albedo are found in all the three months. In fact, the great decrease in planetary albedo in March in past decades coincides with the remarkable reduction in COD (Figure 3g). In other words, the greater annual decline of the runoff in March is closely associated with the larger suppression of cloud formation/development. As such, the cloud influence could be regarded as an additional factor driving the decline of runoff in March on top of global warming, i.e., the COD reduction leads to extra warming at surface, which in turn induce excess evapotranspiration and thereby excess losses of water resource in the basin in March. In contrast, the decreasing of the runoff in February and April appears mainly due to the global warming effect alone.

Although the larger runoff decline in the UCRB in March is not directly associated with the general global warming effect, the stronger subsidence in March leading to the drier and warmer atmosphere which is unfavorable for cloud formation is likely associated with the abnormal circulation patterns in past decades under climate changes. For example, *Kirk et al.* [2017] found that strong ridge patterns along with similar dry patterns have been increasingly common in the spring and early summer, contributing to the early 21st century drought across western North America including the UCRB. Several hypotheses have been proposed to elaborate the dynamical mechanisms of the enhanced likelihood of ridge frequency and persistency over the western United States [*Burgdorf et al.*, 2019; *Kirk and Schmidlin*, 2018; *Namias*, 1983]. One of them argues that the Arctic amplification because of rapid Arctic warming contributes to slower zonal propagation of weather patterns, which is attributable to weakened zonal winds, allowing ridges lingering over certain regions for longer time [*Francis and Vavrus*, 2015; *Kirk and Schmidlin*, 2018]. In addition, the reduced zonal winds in the mid-latitude may result in less contributions from orographic lift to precipitation production in the western United States. Another possible mechanism is related to the poleward shift of subtropical jet stream that is associated with tropical expansion under global warming [*Burgdorf et al.*, 2019]. The poleward-shifted jet accompanies the establishment of ridge control over the western United States, which contributes to the subsidence condition over the

region and thereby suppressing cloud formation. However, all these hypotheses mentioned here still need further in-depth studies from both observational and modeling perspectives in the future.

5. Conclusions

Using multiple datasets from in-situ observations, reanalysis, and modeling, surface and atmospheric variables in the UCRB are analyzed in terms of trend, correlation coefficient, and multiyear monthly mean to examine the recent hydroclimate changes, particularly for the declining runoff in early spring (i.e., February, March and April), given that more than half of the annual mean runoff decline from 1980 to 2018 results from decreases in early spring and that the maximum runoff normally occurs in March. Our analysis shows that the statistically significant annual trends of hydroclimatic parameters are much stronger in March than February and April. This is because, besides the temperature increase associated with global warming, the decrease of COD contributes to the larger decreasing trend of the UCRB runoff in March through its effects on both temperature and precipitation. Multiple linear regression analysis indicates that 25% of the variation of runoff can be explained by COD reduction in March, suggesting that the changes in cloud can exert an additional effect on the runoff on the top of global warming. The recent cloud reduction is likely attributed to the changes in large-scale atmospheric circulations in a changing climate. The abnormal circulation patterns in March tend to cause stronger or persistent ridge control over southwestern United States, contributing to strong subsidence and moisture divergence over the UCRB, thereby suppressing cloud formation. The cloud influence proposed in this study is able to fill the knowledge gap in understanding sub-seasonal variations of hydroclimate in the UCRB. Our analysis also indicates that further studies may be required to understand the abnormal circulation patterns in the changing climate at sub-seasonal level.

Data Availability Statement

The Global Land Data Assimilation System (GLDAS) runoff data was used in this work, which can be downloaded from https://disc.gsfc.nasa.gov/datasets/GLDAS_CLM10_M_V001/sum

KNMI temperature data can be accessed via https://climexp.knmi.nl/selectstation.cgi?id=someone@somewhere
The precipitation and soil moisture data were downloaded from Climate Prediction Center (CPC) via https://www.esrl.noaa.gov/psd/data/gridded/data.unified.html.
Snow water equivalent (SWE) was obtained from Canadian Meteorological Centre (CMC), which can be accessed via https://nsidc.org/data/nsidc-0447.
All other parameters including SW+LW, COD, ALB, Z500hPa, and 3D temperature, water vapor, relative humidity, and wind speeds, were obtained from MERRA-2 via https://disc.gsfc.nasa.gov/datasets/M2TMNXGLC_V5.12.4/summary?keywords=%22MERRA-2%22.

References

https://doi.org/10.1016/0022-1694(86)90199-X

https://doi.org/10.1016/0022-1694(91)90030-L

Ban, Z., T. Das, D. Cayan, M. Xiao, and D. P. Lettenmaier (2020), Understanding the Asymmetry of Annual Streamflow Responses to Seasonal Warming in the Western United States, *Water Resour. Res.*, *56*, 1-19, doi:10.1029/2020WR027158.Burgdorf, A. M., S. Brönnimann, and J. r. Franke (2019), Two types of North American droughts related to different atmospheric circulation patterns, in *Climate of the Past*, edited, pp. 2053-2065, Copernicus GmbH, doi:10.5194/cp-15-2053-2019.Das, T., D. W. Pierce, D. R. Cayan, J. A. Vano, and D. P. Lettenmaier (2011), The importance of warm season warming to western U.S. streamflow changes, *Geophys. Res. Lett.*, *38*, doi:10.1029/2011GL049660.Dawadi, S., and S. Ahmad (2013), Evaluating the impact of demand-side management on water resources under changing climatic conditions and increasing population, *J. Environ. Manage.*, *114*, 261-275, doi:10.1016/j.jenvman.2012.10.015.Engström, A., and A. M. L. Ekman (2010), Impact of meteorological factors on the correlation between aerosol optical depth and cloud fraction, in *Geophys. Res. Lett.*, edited, Blackwell Publishing Ltd, doi:10.1029/2010GL044361.Francis, J. A., and S. J. Vavrus (2015), Evidence for a wavier jet stream in response to rapid Arctic warming, in *Environ. Res. Lett.*, edited, Institute of Physics Publishing, doi:10.1088/1748-9326/10/1/014005.Gleick, P. H. (1986), Methods for evaluating the regional hydrologic impacts of global climatic changes, in *J. Hydrol.*, edited, pp. 97-116, doi:.Halimi, M., M. Rezaei, C. Mohammadi, and M. Farajzadeh (2017), Association between cloudiness and rainfall over Fars province in Iran, in *Russ. Meteorol. Hydrol.*, edited, pp. 671-676, Allerton Press Incorporation, doi:10.3103/S1068373917100077.Hamlet, A. F., P. W. Mote, M. P. Clark, and D. P. Lettenmaier (2007), Twentieth-century trends in runoff, evapotranspiration, and soil moisture in the western United States, in *J. Clim.*, edited, pp. 1468-1486, doi:10.1175/JCLI4051.1.Hardle, W. K., and L. Simar (2015), Applied Multivariate Statistical Analysis, edited, Springer, Berlin, Germany.Hobbins, M., and J. Barsugli (2020), Threatening the vigor of the Colorado River, in *Science (New York, N.Y.)*, edited, pp. 1192-1193,

doi:10.1126/science.abb3624.Hock, R., G. Rasul, C. Adler, B. Cáceres, S. Gruber, Y. Hirabayashi, M. Jackson, A. Kääb, S. Kang, S. Kutuzov, Al. Milner, U. Molau, S. Morin, B. Orlove, and H. Steltzer (2019), High Mountain Areas. In: IPCC Special Report on the Ocean and Cryosphere in a Changing Climate*Rep.*, IPCC, Genf, Switzerland.Hoerling, M., J. Barsugli, B. Livneh, J. Eischeid, X. Quan, and A. Badger (2019), Causes for the century-long decline in Colorado river flow, in *J. Clim.*, edited, pp. 8181-8203, doi:10.1175/JCLI-D-19-0207.1.Huntington, T. G., and M. Billmire (2014), Trends in precipitation, runoff, and evapotranspiration for rivers draining to the gulf of Maine in the United States, in *J. Hydrometeorol.*, edited, pp. 726-743, American Meteorological Society, doi:10.1175/JHM-D-13-018.1.Johnson, R. A., and D. W. Wichern (2007), Applied multivariate statistical analysis, edited, Pearson Education Inc, NJ.Karl, T. R., and W. E. Riebsame (1989), The impact of decadal fluctuations in mean precipitation and temperature on runoff: A sensitivity study over the United States, in *Clim. Change*, edited, pp. 423-447, doi:10.1007/BF00240466.Kirk, J. P., and T. W. Schmidlin (2018), Moisture transport associated with large precipitation events in the Upper Colorado River Basin, in *Int. J. Climatol.*, edited, pp. 5323-5338, doi:10.1002/joc.5734.Kirk, J. P., S. C. Sheridan, and T. W. Schmidlin (2017), Synoptic climatology of the early 21st century drought in the Colorado River Basin and relationships to reservoir water levels, in *Int. J. Climatol.*, edited, pp. 2424-2437, John Wiley and Sons Ltd, doi:10.1002/joc.4855.Lamquin, N., C. J. Stubenrauch, and J. Pelon (2009), Upper tropospheric humidity and cirrus geometrical and optical thickness: Relationships inferred from 1 year of collocated AIRS and CALIPSO data, in *J. Geophys. Res.*, edited, pp. 1-12, doi:10.1029/2008JD010012.Lehner, F., C. Deser, I. R. Simpson, and L. Terray (2018), Attributing the U.S. Southwest's Recent Shift Into Drier Conditions, in *Geophys. Res. Lett.*, edited, pp. 6251-6261, Blackwell Publishing Ltd, doi:10.1029/2018GL078312.Liu, C., et al. (2017), Continental-scale convection-permitting modeling of the current and future climate of North America, in *Clim. Dyn.*, edited, pp. 71-95, Springer Berlin Heidelberg, doi:10.1007/s00382-016-3327-9.Mavromatis, T., and D. Stathis (2011), Response of the water balance in Greece to temperature and precipitation trends, in *Theor. Appl. Climatol.*, edited, pp. 13-24, Springer-Verlag Wien, doi:10.1007/s00704-010-0320-9.McCabe, G. J., D. M. Wolock, G. T. Pederson, C. A. Woodhouse, and S. McAfee (2017), Evidence that recent warming is reducing upper Colorado river flows, in *Earth Interact.*, edited, American Meteorological Society, doi:10.1175/EI-D-17-0007.1.Miller, W. P., and T. C. Piechota (2008), Regional Analysis of Trend and Step Changes Observed in Hydroclimatic Variables around the Colorado River Basin, in *J. Hydrometeorol.*, edited, pp. 1020-1034, American Meteorological Society, Boston MA, USA, doi:10.1175/2008JHM988.1.Milly, P. C. D., and K. A. Dunne (2020), Colorado River flow dwindles as warming-driven loss of reflective snow energizes evaporation, in *Science*, edited, pp. 1252-1255.Milly, P. C. D., J. Kam, and K. A. Dunne (2018), On the Sensitivity of Annual Streamflow to Air Temperature, in *Water Resour. Res.*, edited, pp. 2624-2641, Blackwell Publishing Ltd, doi:10.1002/2017WR021970.Mishra, A.

K. (2019), Investigating changes in cloud cover using the long-term record of precipitation extremes, in *Meteorol. Appl.*, edited, pp. 108-116, John Wiley and Sons Ltd, doi:10.1002/met.1745.Namias, J. (1983), Some Causes of United States Drought, in *J. Appl. Meteorol. Climatol.*, edited, pp. 30-39.Nash, L. L., and P. H. Gleick (1991), Sensitivity of streamflow in the Colorado Basin to climatic changes, in *J. Hydrol.*, edited, pp. 221-241, doi:.Nowak, K., M. Hoerling, B. Rajagopalan, and E. Zagona (2012), Colorado river basin hydroclimatic variability, in *J. Clim.*, edited, pp. 4389-4403, doi:10.1175/JCLI-D-11-00406.1.Painter, T. H., J. S. Deems, J. Belnap, A. F. Hamlet, C. C. Landry, and B. Udall (2010), Response of Colorado River runoff to dust radiative forcing in snow, in *Proc. Nat. Acad. Sci. U.S.A.*, edited, doi:10.1073/pnas.0913139107.Pascolini-Campbell, M., J. T. Reager, H. A. Chandanpurkar, and M. Rodell (2021), A 10 per cent increase in global land evapotranspiration from 2003 to 2019, in *Nature*, edited, pp. 543-547, Nature Research, doi:10.1038/s41586-021-03503-5.Sakakibara, H. (1978), NOTES AND CORRESPONDENCE Statistical Relations between Precipitation Formation and Quantities of Synoptic Field.Seneviratne, S. I., T. Corti, E. L. Davin, M. Hirschi, E. B. Jaeger, I. Lehner, B. Orlowsky, and A. J. Teuling (2010), Investigating soil moisture-climate interactions in a changing climate: A review, in *Earth Sci. Rev.*, edited, pp. 125-161, doi:10.1016/j.earscirev.2010.02.004.Smith, R. A., and C. D. Kummerow (2013), A comparison of in situ, reanalysis, and satellite water budgets over the upper colorado river basin, in *J. Hydrometeorol.*, edited, pp. 888-905, doi:10.1175/JHM-D-12-0119.1.Udall, B., and J. Overpeck (2017), The twenty-first century Colorado River hot drought and implications for the future, in *Water Resour. Res.*, edited, pp. 2404-2418, doi:10.1002/2016WR019638.Received.USGS (2016), Colorado River Basin map, https://www.usgs.gov/media/images/colorado-river-basin-map.Vano, J. A., T. Das, and D. P. Lettenmaier (2012), Hydrologic sensitivities of Colorado River runoff to changes in precipitation and temperature, in *J. Hydrometeorol.*, edited, pp. 932-949, doi:10.1175/JHM-D-11-069.1.Vano, J. A., and D. P. Lettenmaier (2014), A sensitivity-based approach to evaluating future changes in Colorado River discharge, in *Clim. Change*, edited, pp. 621-634, Kluwer Academic Publishers, doi:10.1007/s10584-013-1023-x.Vano, J. A., B. Nijssen, and D. P. Lettenmaier (2015), Seasonal hydrologic responses to climate change in the Pacific Northwest, in *Water Resour. Res.*, edited, pp. 1959-1976, Blackwell Publishing Ltd, doi:10.1002/2014WR015909.Walcek, C. J. (1994), Cloud Cover and Its Relationship to Relative Humidity during a Springtime Midlatitude Cyclone, in *Mon. Weather Rev.*, edited, pp. 1021-1035, American Meteorological Society, Boston MA, USA, doi:10.1175/1520-0493(1994)122<1021:CCAIRT>2.0.CO;2.Wigley, T. M. L., and P. D. Jones (1985), Influences of precipitation changes and direct CO2 effects on streamflow, *Nature*, *314*(6007), 149-152, doi:10.1038/314149a0.Woodhouse, C. A., G. T. Pederson, K. Morino, S. A. McAfee, and G. J. McCabe (2016), Increasing influence of air temperature on upper Colorado River streamflow, in *Geophys. Res. Lett.*, edited, pp. 2174-2181, doi:10.1002/2015GL067613.Xiao, M., B. Udall, and D. P. Lettenmaier (2018), On the Causes of Declining Colorado

River Streamflows, in *Water Resour. Res.*, edited, pp. 6739-6756, Blackwell Publishing Ltd, doi:10.1029/2018WR023153.Yue, S., and C. Wang (2004), The Mann-Kendall Test Modified by Effective Sample Size to Detect Trend in Serially Correlated Hydrological Series, paper presented at Water Resour. Manage.Zhao, B., Y. Gu, K. N. Liou, Y. Wang, X. Liu, L. Huang, J. H. Jiang, and H. Su (2018), Type-Dependent Responses of Ice Cloud Properties to Aerosols From Satellite Retrievals, in *Geophys. Res. Lett.*, edited, pp. 3297-3306, Blackwell Publishing Ltd, doi:10.1002/2018GL077261.Zhao, S., R. Fu, Y. Zhuang, and G. Wang (2021), Long-Lead Seasonal Prediction of Streamflow over the Upper Colorado River Basin: The Role of the Pacific Sea Surface Temperature and Beyond, *J. Clim.*, *34*, 6855-6873 doi:10.1175/JCLI-D-20.

Figure 1 Map of upper Colorado River basin (UCRB). A red frame indicates the investigated domain: 35-43° N, 105.7-111° W. (source: https://www.usgs.gov/media/images/colorado-river-basin-map).

Figure 2 (a) Multiyear monthly mean of runoff, temperature, precipitation, and snow water equivalent (SWE) averaged over the UCRB. The primary runoff peak occurs in March. (b) The time series of annual UCRB runoff curve (left axis) and its anomalies in stack bars (right axis) with respective to (1980-2018) mean. The contributions of February, March, and April to annual total runoff anomaly are marked as green, red, and blue bars, respectively.

Figure 3 Time series of monthly (a) runoff, (b) surface temperature, (c) precipitation, (d) soil moisture, (e) surface net radiative flux, (f) snow water equivalent (SWE), and (g) cloud optical depth (COD), and in the UCRB in February (green dash), March (red dash), and April (blue dash), and their annual trend fittings (thick solid lines) during 1980-2018. Numbers in each panel denote the Theil-Sen slopes of linear fittings, with the asterisks denoting that trends pass the Mann-Kendall trend significance test at the of 0.05 (*) or 0.10 (**) level.

Figure 4 (a) Linear regression between cloud optical depth (COD) and relative humidity (RH) with 95% confidence limits (grey shading) and 95% prediction limits (dash lines), and time series of column mean (1000 ~ 300 hPa) (b) RH and (c) temperature in UCRB in February (green), March (red), and April (blue), and their trends (thick solid lines) for the period 1980 – 2018. Numbers in (b) and (c) denote the Theil-Sen slopes of linear fittings, with the asterisks denoting that the linear trend passes the Mann-Kendall trend significance test at the of 0.05 level. Green, red and blue colors in all panels represent February, March, and April, respectively. **Figure 5** The difference between the last ten years (2009-2018) and the first ten years (1980-1989) in (a) geopotential height at 500 hPa (Z_{500}, shading) superimposed with wind vectors at same level, (b) vertical velocity (, shading) along latitude-height cross section over UCRB superimposed with vectors of (V component of wind, -), and (c) vertically integrated moisture flux divergence (1000 ~ 300 hPa, shading) over UCRB domain superimposed with vertically integrated moisture flux (1000 ~ 300 hPa, vectors). The

green boxes in (a) mark the UCRB domain, which is domain used for analysis in (b) and (c). From left to right in each panel are February, March and April. The UCRB domain-mean moisture flux divergence for each month is marked in (c), which are yellow-highlighted.

Figure 6 Time series of domain-mean (a) geopotential height at 500 mb and (b) vertically integrated moisture flux divergence over UCRB in February (green dash), March (red dash), and April (blue dash), and their trend (thick solid lines) for the period 1980 – 2018.

Figure 7 Flow diagram for the causative relationships among large-scale circulation characteristics, cloud optical depth, and hydroclimatic variables (including runoff) in the UCRB in early spring of 1980-2018 (except 1999-2018 for SWE) under varying climate. Red and blue arrows denote increasing and decreasing trends, respectively. The key factors cloud optical depth, temperature, precipitation and runoff are highlighted in bold. The background grey giant arrow suggests that all the changes are originated from abnormal circulation patterns under changing climate. For February and April, the hydroclimatic response is encompassed in the dashed box, as it starts from variations of surface temperature and precipitation which are likely resulted from climatic warming alone.

Table 1 Correlation coefficient and partial correlation coefficient between UCRB variables of runoff (RO), temperature, precipitation, and could optical depth (COD) (1980 – 2018). $R_{A,B}$ is correlation coefficient between A and B. $R_{(A,B)\,C}$ is partial correlation coefficient between A and B while controlling the effect of C.